Published in final edited form as:
J Med Chem. 2010 February 11; 53(3): 1329. doi:10.1021/jm901624n.

Catalysis and inhibition of *Mycobacterium tuberculosis* methionine aminopeptidase

Jing-Ping Lu, **Sergio C. Chai**, and **Qi-Zhuang Ye***
Department of Biochemistry and Molecular Biology, Indiana University School of Medicine, Indianapolis, Indiana 46202

Abstract

Methionine aminopeptidase (MetAP) carries out an important cotranslational N-terminal methionine excision of nascent proteins and represents a potential target to develop antibacterial and antitubercular drugs. We cloned one of the two MetAPs in *Mycobacterium tuberculosis* (*Mt*MetAP1c from the *mapB* gene) and purified it to homogeneity as an apoenzyme. Its activity required a divalent metal ion, and Co(II), Ni(II), Mn(II) and Fe(II) were among activators of the enzyme. Co(II) and Fe (II) had the tightest binding, while Ni(II) was the most efficient cofactor for the catalysis. *Mt*MetAP1c was also functional in *E. coli* cells, because a plasmid-expressed *Mt*MetAP1c complemented the essential function of MetAP in *E. coli* and supported the cell growth. A set of potent *Mt*MetAP1c inhibitors were identified, and they showed high selectivity towards the Fe(II)-form, the Mn(II)-form, or the Co(II)- and Ni(II)-forms of the enzyme, respectively. These metalloform selective inhibitors were used to assign the metalloform of the cellular *Mt*MetAP1c. The fact that only the Fe(II)-form selective inhibitors inhibited the cellular *Mt*MetAP1c activity and inhibited the *Mt*MetAP1c-complemented cell growth suggests that Fe(II) is the native metal used by *Mt*MetAP1c in an *E. coli* cellular environment. Finally, X-ray structures of *Mt*MetAP1c in complex with three metalloform-selective inhibitors were analyzed, which showed different binding modes and different interactions with metal ions and active site residues.

Introduction

Tuberculosis (TB) is a deadly disease caused by mycobacterial infection, and *Mycobacterium tuberculosis* is the major pathogen for TB in humans. Now, multidrug-resistant and extensively drug-resistant TB is happening at an alarming rate.[1] To overcome the drug resistance, new antibiotics with novel mechanisms of action are urgently needed. Methionine aminopeptidase (MetAP) is a ubiquitous enzyme found in both prokaryotic and eukaryotic cells and carries out an important posttranslational modification of newly synthesized proteins. Therefore, MetAP is a promising target for developing novel drugs against bacterial infection, including TB-causing drug-resistantbacteria.[2]

Every protein is expressed with a methionine at its N-terminus, and about 50-70% of nascent proteins undergo N-terminal methionine excision, which is required for localization, activation, and degradation.[3] Eukaryotic cells express two MetAPs, type 1 and type 2. The two subtypes of MetAP are homologous, and type 2 MetAP has an extra insert in the catalytic domain. In contrast, prokaryotic cells usually only express one MetAP. Eubacteria only have a type 1 MetAP, while archaea only have a type 2 MetAP. Multiple MetAPs are rare in bacteria, but

*To whom correspondence should be addressed: Department of Biochemistry and Molecular Biology, Indiana University School of Medicine, 635 Barnhill Drive, Indianapolis, IN 46202. Tel.: 317-278-0304; Fax: 317-278-4686; yeq@iupui.edu.
PDB ID Codes: 3IU7, 3IU8, and 3IU9

with more genomic sequences reported, two or more putative MetAP genes have been identified in a small number of bacteria. So far, twenty genomes of mycobacteria have been sequenced, and putative MetAP proteins in each mycobacterial genome, ranging from two to four, were identified by sequence analysis. For example, *M. tuberculosis* has two MetAP genes (*mapA* and *mapB* in H37Rv genome and *map_1* and *map_2* in CDC1551 genome), and both belong to type 1 MetAP with high homology to *E. coli* MetAP (*Ec*MetAP). For most of these putative MetAPs, little is known about their biochemical properties beyond their sequences. The protein from *mapB* gene of *M. tuberculosis*, named *Mt*MetAP1c, was purified, and its structures in apoform and in complex with methionine were reported.[4] The structural analysis revealed a SH3 binding motif at its N-terminus, and potential interaction with ribosome through the motif to facilitate cotranslational methionine excision was proposed.[4] The other MetAP (from *mapA* gene) of *M. tuberculosis*, named *Mt*MetAP1a, is shorter at the N-terminus and has no such SH3 binding motif.

MetAP is one of the dinuclear metallohydrolases,[5-6] and divalent metal ions play a key role in the hydrolysis catalyzed by MetAP. When purified as an apoenzyme, MetAP can be activated by several divalent metals, including Co(II), Mn(II), and Fe(II).[7-8] Initially, MetAP was believed to be a Co(II) enzyme, because Co(II) is among the best activators, and early X-ray structures of MetAP all contained two Co(II) ions at the active site.[9] Most of the currently known MetAP inhibitors were discovered and characterized with MetAP in the Co(II)-form. However, it is puzzling that many current small molecule MetAP inhibitors with high potencies on purified enzymes failed to show any significant antibacterial activity.[10-12] We confirmed that inhibitors of the Co(II)-form may not inhibit other metalloforms of MetAP.[8, 13] There are many reasons that an *in vitro* active compound may be inactive *in vivo*, such as absorption or metabolism. However, one explanation for the lack of antibacterial activities may be a disparity between the metalloform tested using a purified enzyme and the one that exists in cells. It is apparent that MetAP inhibitors have to effectively inhibit the cellular MetAP to be therapeutically useful. We have developed several sets of metalloform-selective MetAP inhibitors based on high throughput screening hits,[13-14] and these inhibitors can inhibit either Co(II)-, Mn(II)- or Fe(II)-form of *Ec*MetAP with both high potency and selectivity. We used these metalloform-selective MetAP inhibitors to characterize inhibition of purified *Ec*MetAP and inhibition of cellular MetAP in *E. coli*. The fact that only Fe(II)-form selective inhibitors showed antibacterial activity on several *E. coli* and *Bacillus* strains led us to conclude that Fe (II) is the likely metal used by MetAP in *E. coli* and other bacterial cells.[15]

Characterization of catalysis and inhibition of mycobacterial MetAPs is a necessary step in discovery and development of their inhibitors. However, enzymatic activity of *Mt*MetAP1a and *Mt*MetAP1c was reported only recently by overexpressing the proteins in *E. coli*.[16] Both of the recombinant *M. tuberculosis* MetAP enzymes were soluble and active when purified, and the activity was enhanced by Co(II) and inhibited by Cu(II), Fe(II) and Ni(II).[16] Apparently, the MetAP proteins were purified with metal already incorporated. We independently expressed *Mt*MetAP1c in *E. coli* and purified it to homogeneity as an apoenzyme. Contrary to what was reported,[16] we found that Ni(II) and Fe(II) were excellent activators of the purified apoenzyme. Further, we demonstrated that it was a functional MetAP in *E. coli* cells. No inhibitors have been described for mycobacterial MetAPs. Here, we report the characterization of several metalloform-selective inhibitors for inhibition of both purified *Mt*MetAP1c and the enzyme in an *E. coli* cellular environment and present the first inhibited structures of *Mt*MetAP1c in complex with three metalloform-selective inhibitors.

Results

Expression and purification of *Mt*MetAP1c protein

The expression plasmid for *Mt*MetAP1c was constructed by PCR amplification of *mapB* gene in *M. tuberculosis* H37Rv strain as an *Nhe*I and *Eco*RI fragment and insertion of the fragment into an expression vector pGEMEX1 for a T7-promoter controlled expression in *E. coli*. Only three extra amino acid residues MAS were added to its N-terminus for cloning purposes. No attempt was made to remove the extra sequence, although the terminal methionine is often processed cotranslationally by MetAP in *E. coli* cells.[31] The protein was expressed at a high level as a soluble and active protein, and it was purified easily to homogeneity as an apoenzyme in high yield (20 to 30 mg/liter cell culture). The apoenzyme showed no activity when tested by the fluorogenic substrate Met-AMC and could be activated by divalent metals instantly.

Activation of *Mt*MetAP1c apoenzyme by divalent metals

It is common for a purified metalloenzyme to be activated by several different metal ions. For example, *Ec*MetAP can be activated by Co(II), Ni(II), Mn(II), Fe(II) and Zn(II).[7] Similar sizes of these metal ions make this isomorphous replacement possible. We tested *Mt*MetAP1c for activation by divalent metals, including Co(II), Ni(II), Mn(II), Fe(II) and Zn(II) (Fig. 1). The bell-shaped metal activation curves were observed, and similar curves were observed previously with *Ec*MetAP.[8] High concentrations of a metal often inhibit MetAP enzymatic activity. Co(II) activated *Mt*MetAP1c effectively, starting at a low concentration less than 1 μM, consistent with its activation for many MetAPs.[8] What is unique and surprising is the observed strong activation of *Mt*MetAP1c by Ni(II), because this has not been observed in *Ec*MetAP or other MetAPs, and this contradicts the belief that bacterial MetAPs use Fe(II) as their native cofactor.[7, 15] This raises the question whether Ni(II) is the native cofactor for *Mt*MetAP1c. Mn(II) and Fe(II) also showed activation, while no activation was observed for Zn(II).

Kinetic characterization of metal binding and activation of *Mt*MetAP1c

To further understand the metal binding and activation of *Mt*MetAP1c, we carried out detailed kinetic studies with the activating metal ions. The hydrolysis of Met-AMC can be conveniently monitored by fluorescence from the released aminomethylcoumarin. Holding the amount of *Mt*MetAP1c apoenzyme and substrate Met-AMC constant, we calculated the affinity (K_d) for each of the activating metals by fitting a model of multiple independent binding sites, taking into consideration the amount of functional enzyme.[20] It is apparent that Co(II) and Fe(II) bound to *Mt*MetAP1c the tightest with the lowest K_d values, followed by Mn(II) (Table 1). Ni (II) was shown to have the weakest affinity, which is about 10 fold weaker than Fe(II) or Co (II). At the optimal activating metal concentrations, Michaelis–Menten constants were calculated. Interestingly, Ni(II)-activated *Mt*MetAP1c was the most efficient among the metalloforms tested in catalyzing the hydrolysis of the substrate, with the lowest K_m and the fastest k_{cat}, consistent with the metal titration curve (Fig. 1).

Complementation of function of *Ec*MetAP by *Mt*MetAP1c in *E. coli* cells

A functional MetAP enzyme is essential for *E. coli* growth,[32] and the *Ec*MetAP gene cannot be removed. However, an *E. coli* strain with an amber mutation at its chromosomal *Ec*MetAP gene was constructed.[18, 21] This *E. coli* strain carries a plasmid with a pBAD-regulated amber suppressor tRNA gene, and expression of the tRNA suppresses the lethal effect of the amber mutation.[18] The *E. coli* cells grow in the presence of arabinose, because expression of the tRNA is induced, and a functional *Ec*MetAP is produced. On the other hand, the cells do not grow in the presence of glucose, because no such tRNA is expressed and a truncated and inactive *Ec*MetAP is produced due to the amber mutation not being suppressed. Function of the

chromosomally expressed *Ec*MetAP can be complemented with a functional MetAP expressed from a plasmid. To test whether *Mt*MetAP1c can function in an *E. coli* cellular environment, we constructed such a plasmid by putting the *Mt*MetAP1c gene behind an IPTG-inducible *tac* promoter in pFLAGCTC plasmid as pFLAGCTC-*Mt*MetAP1c and transformed the *E. coli* cells. As controls, parent plasmid pFLAGCTC, which expresses no MetAP, and the plasmid pFLAGCTC-*Ec*MetAP, which expresses *Ec*MetAP, were also used for the transformation. On agar plates, we observed that the cells transformed with pFLAGCTC grew in the presence of arabinose and did not grow in the presence of glucose (Fig. 2A), confirming the requirement for a functional MetAP for growth. The cells with either pFLAGCTC-*Ec*MetAP or pFLAGCTC-*Mt*MetAP1c grew on the agar plate in the absence of arabinose and presence of glucose (Fig. 2A), which suggests that *Ec*MetAP or *Mt*MetAP1c expressed from the plasmids was functional and complemented the function of chromosomally expressed *Ec*MetAP to support the growth. We also tested the growth of the transformed *E. coli* strains in a liquid medium supplemented with glucose and without arabinose. The cells with either pFLAGCTC-*Ec*MetAP or pFLAGCTC-*Mt*MetMetAP1c showed robust growth, while the *E. coli* cell with the parent plasmid pFLAGCTC did not grow under the same conditions (Fig. 2B). These results confirm that *Mt*MetAP1c expressed from a plasmid in *E. coli* was a functional enzyme and supported the growth of *E. coli* cells when *Ec*MetAP was absent.

Metalloform-selective inhibition of purified *Mt*MetAP1c and the enzyme in an *E. coli* cellular environment

A set of inhibitors (Table 2) with known metalloform-selectivity for *Ec*MetAP were used to evaluate inhibition of purified *Mt*MetAP1c enzyme and the same enzyme in an *E. coli* cellular environment, to provide clues for the metal cofactor used by *Mt*MetAP1c in cells. The catechol compounds **1** and **2** inhibited selectively the Fe(II) form of *Ec*MetAP,[14] while **3** and **4** were shown to be highly selective inhibitors for the Mn(II) form.[13] Triazole inhibitors were shown to interact directly with the catalytic metal ions through nitrogen atoms,[33] and we predicted their preference for the Co(II) and Ni(II) forms of MetAP because of their chelation through nitrogen atoms.[34] We selected four such triazole compounds, **5**-**8**, for this study. All of the eight MetAP inhibitors were first tested with purified *Mt*MetAP1c apoenzyme activated by Co (II), Ni(II), Mn(II) or Fe(II). Indeed, all of these inhibitors showed potent and metalloform-selective inhibition at low micromolar or submicromolar concentrations (Table 2). **1** and **2** were selective for the Fe(II) form, **3** and **4** were selective for the Mn(II) form, and **4**-**8** were selective for the Ni(II) and Co(II) forms. Subsequently, we tested some of them for their ability to inhibit the cellular enzymatic activity of *Mt*MetAP1c in permeabilized *E. coli* cells. Inclusion of Ca(II) at 5 mM made these cells permeable to substrates and inhibitors, and Ca(II) had no effect on MetAP activity.[15] Clearly, the highest inhibition of the cellular *Mt*MetAP1c activity was achieved by the two Fe(II)-form selective inhibitors **1** and **2** (Table 2), suggesting that *Mt*MetAP1c present in the live *E. coli* cells used Fe(II), not Ni(II) or Co(II), as the cofactor for catalysis.

Growth inhibition of *Mt*MetAP1c-complemented *E. coli* cells

The N-terminal methionine excision is an important co-translational process, and a lethal phenotype was observed when the single gene coded for *Ec*MetAP was deleted in *E. coli*,[32] demonstrating its essentiality for bacterial survival. In our construct, *Mt*MetAP1c complements the essential function of *Ec*MetAP in *E. coli* cells. Therefore, effective inhibition of cellular *Mt*MetAP1c will conceivably inhibit the growth of the *E. coli* cells. We tested the metalloform-selective inhibitors on the *E. coli* cells with *Mt*MetAP1c complementation and observed that only the Fe(II)-form selective inhibitors **1** and **2** proved to arrest bacterial cell growth (Table 2). In contrast, inhibitors **3**, **5** and **6** showed no inhibition at the highest concentration (1 mM) tested, indicating that they could not inhibit the cellular *Mt*MetAP1c. Although it is still possible that **3**, **5** and **6** could not penetrate the permeabilized cell walls, the observed inhibition

by **1** and **2** is consistent with the conclusion that the functional metalloform of cellular *Mt*MetAP1c exists as the Fe(II)-form. We have previously demonstrated that **1** and **2** prevented *E. coli* growth by directly targeting *Ec*MetAP, as observed by monitoring the retention of the N-terminal methionine in the biomarker glutathione-S-transferase.[15]

X-ray structures of *Mt*MetAP1c in complex with inhibitors

Structural information for mycobacterial MetAPs is lacking, and only two X-ray structures of *Mt*MetAP1c either as an apoenzyme or in complex with product methionine were reported.[4] With the confirmed inhibition of *Mt*MetAP1c by our metalloform selective inhibitors, we embarked on crystallization and structural analysis to elucidate their binding mode at the active site of *Mt*MetAP1c. Three structures of such enzyme-inhibitor complexes with either **4**, **7**, or **8** were obtained independently. All of the structures were folded in the "pita-bread" shape commonly seen in MetAP structures.[9] Electron density for two metal ions was clearly observed at the dinuclear metal site, and the inhibitors bound in the shallow and mostly hydrophobic active site pocket.

It is interesting that all of our three structures showed $P6_3$ space group in the crystal packing, instead of the common $P2_1$ space group for other MetAPs. This symmetry indicates a trimeric arrangement in the crystals (Fig. 3A), and indeed, the calculation on the PISA server (Protein interfaces, surfaces and assemblies service, http://www.ebi.ac.uk/msd-srv/prot_int/pistart.html)35 showed that there are large contact surfaces between the protein molecules, and a trimetric form is energetically favored. However, similar analysis for the previous *Mt*MetAP1c structures (Pdb codes 1Y1N and 1YJ3, with $P2_1$ space group) yielded no specific interactions between protein molecules, and a monomeric solution structure was predicted. The previously reported *Mt*MetAP1c has a longer N-terminus with a His-tag present,[4] and it is not known whether the extra sequence, although not visible in the X-ray structures, prevented its packing in crystals as a trimer. The His-tag is not located near the contact surfaces. The question is whether *Mt*MetAP1c is trimeric in solution. We eluted our *Mt*MetAP1c (31 kDa predicted molecular weight) in 50 mM Tris, pH 7.5, with 150 mM NaCl through a Superdex 75 size-exclusion column, with blue dextran (2000 kDa), aldolase (153 kDa), bovine serum albumin (67 kDa), ovalbumin (43 kDa), and ribonuclease (13.7 kDa) as molecular weight standards. *Mt*MetAP1c was eluted between ovalbumin and ribonuclease, suggesting a monomeric state in the solution condition. Disagreement in oligomer states between crystal packing and solution has been noted,[36] and it is possible that *Mt*MetAP1c exists in a trimeric form in some crystals, while it is monomeric in solution.

X-ray structure of *Mt*MetAP1c in complex with 4 in the Mn(II)-form

The structure was solved to 1.4 Å resolution, and two molecules of **4** were fitted to the structure. One of the inhibitor molecules occupied the active site, and the other took a position on the opposite side of the protein molecule, 10.9 Å away from the active site inhibitor. The structure of *Ec*MetAP in complex with the same inhibitor was solved before (pdb code 1XNZ), and only one inhibitor molecule was identified.[13] When these two structures were overlaid, the active site inhibitor showed the same binding mode with a non-coplanar conformation between its two aromatic rings (Fig. 3B). Occupation of **4** at the active site is likely sufficient for MetAP inhibition, because the second molecule of **4** was not observed in the *Ec*MetAP structure, and **4** inhibited both *Mt*MetAP1c and *Ec*MetAP potently at 16 μM and 0.24 μM,[13] respectively. *Ec*MetAP has a longer C-terminus, and the binding of a second **4** is spatially incompatible with residues R251, D253 and D254 in *Ec*MetAP.

The previous *Mt*MetAP1c structure (pdb code 1YJ3) is in the Co(II) form, and the ligand used is also different. However, superimposing the two structures by aligning all main chain atoms from residue R4 to the end residue L285 gave a rmsd of 0.301 Å, indicating very similar

structures. Due to different ligands, the active site residues showed movements to accommodate the different sizes of the ligands. The most significant movements were H114, which moved by 1.4 Å and is a conserved residue in *Ec*MetAP that plays an important role in catalysis,[37] and W255, which moved the most by 2.2 Å.

X-ray structures of *Mt*MetAP1c in complex with 7 or 8 in the Ni(II)-form

Triazoles were reported as potent inhibitors of the Co(II)-form of *Staphylococcus aureus* MetAP (IC_{50}, 43.7 nM),[33] and X-ray structures of enzyme-inhibitor complexes were reported. Here we described the inhibition of *Mt*MetAP1c by similar triazole compounds with high potency at submicromolar concentrations and selectivity for the Co(II) and Ni(II)-form. We crystallized two of the triazole inhibitors (**7** and **8**) with *Mt*MetAP1c in a unique Ni(II)-form and solved the complexes to 1.85 Å and 1.75 Å resolution, respectively. Although both inhibitors have the same triazole moiety, they bound differently at the active site. While **8** bound at the active site as a dimetalated structure (Fig. 4B), **7** acquired an additional Ni(II) ion to form a trimetalated structure (Fig. 4A). The extra ion was tetra coordinated with ligation to the conserved H144 mentioned before and to a water molecule and a chlorine ion as the third and fourth coordination points. Trimetalated MetAP enzyme in complex with other types of inhibitors have been observed before,[12, 34, 38] and their formation requires specific spatial arrangement of coordinating heteroatoms. However, it is interesting to note that **7** formed a trimetalated structure, while **8** formed a dimetalated structure with small structural differences. These two structures also differ significantly at the dinuclear metal site. M1 and M2 were both pentacoordinated in the complex with **7**, and they became hexacoordinated in the complex with **8**. The distances from M1 to the two oxygen atoms of E238 are 2.0 Å and 3.2 Å in the complex with **7**, therefore, E238 provided only one oxygen atom for coordination. In contrast, the distances are 2.1 Å and 2.2 Å in the other complex, and both oxygen atoms coordinated with M1. For M2 coordination, one of the oxygen atoms of E269 shifted from a monodentate mode to M1 in complex with **7** to a bridging bidentate mode to both M1 and M2 in complex with **8**, providing the additional coordination point for M2.

A unique structural feature of the complex with **8** is the bound conformation of the inhibitor. Although both **7** and **8** have the core benzylthiotriazole structure, **8** adapted a bound conformation, with its benzyl group turning into a pocket formed by rotation of F211 by 90° (Fig. 4C). This binding pocket identified by this structure has not been seen in any other MetAP structures and provides additional interactions for MetAP inhibitor design.

Discussion

Both MetAPs in *M. tuberculosis* were active as enzymes when purified, and their mRNA transcripts were analyzed and showed different levels in the log phase and the stationary phase.[16] The *Mt*MetAP1a gene (*mapA*) expressed more in the log phase, while *Mt*MetAP1c gene (*mapB*) showed a higher level in the stationary phase. It was concluded that the two MetAPs may perform important functions in different growth phases of *M. tuberculosis*.[16] The special characteristics of the mycobacterial life cycle may require more than one MetAP enzyme to carry out the important cotranslational modification. Although the majority of bacteria have only one MetAP gene, two or more MetAP genes were identified in a small number of bacteria, and most of them have not been characterized enzymatically. Two homologous type 1 MetAP isozymes in *Bacillus subtilis* were isolated and investigated.[39] Although both showed enzymatic activity, only one of them was essential for growth, and the other was concluded to be non-essential due to low expression.[39] Two MetAP genes were also identified in *Acinetobacter baumannii*, but none of them has been demonstrated as a functional enzyme. The protozoan parasite *Plasmodium falciparum* has four MetAP sequences, and inhibitors discovered and characterized on one of the four showed antimalarial activity.[40] Deletion of the

single MetAP gene from *E. coli*[32] or *Salmonella typhimurium*[41] is lethal. *Saccharomyces cerevisiae* has two copies of MetAP enzymes, a type 1 and a type 2. Deletion of one of them showed a slow growth phenotype, and deletion of both was required to produce lethality.[42] *Mt*MetAP1a and *Mt*MetAP1c both belong to type 1 MetAP, and an alignment of their protein sequences showed 33% identity.[43] Because *Mt*MetAP1a and *Mt*MetAP1c are very homologous enzymes, it is likely that the function of one can be complemented by the other, and inhibitors of one will inhibit the other as well. Therefore, both *Mt*MetAP1a and *Mt*MetAP1c are potential drug targets, and inhibition of one or both is likely required to show antimycobacterial activity.

We purified *Mt*MetAP1c to homogeneity as an apoenzyme and demonstrated its enzymatic function not only as a purified enzyme but also in live *E. coli* cells. Divalent metals Co(II), Mn (II), Ni(II), and Fe(II) all showed instant activation of the purified apoenzyme. Co(II) and Fe (II) had higher affinities, and Ni(II) bound more weakly but showed the highest catalytic efficiency. Zhang et al.[16] described Fe(II) and Ni(II) as inhibitors of *Mt*MetAP1c activity, contradicting some of our results. However, their enzyme showed high activity before the metal ion was added, indicating that a metalated enzyme was used instead of an apoenzyme. The enzyme was purified as a His-tagged protein, and no procedure was described for metal removal. Their observed inhibitory effect of Fe(II) or Ni(II) was probably due to competition of the metal added with the active site metal already in place. Another possibility is that higher metal concentrations (in addition to the metal already in place) were used in their experiments, and our metal activation profiles (Fig. 1) showed that a metal can also inhibit MetAP activity at high concentrations. It is interesting to note that a MetAP enzyme was purified from *Mycobacterium smegmatis* mc^2155 strain, and its enzymatic activity was enhanced by Mg(II) and Co(II) and inhibited by Fe(II) and Cu(II).[44] However, the enzyme was purified by following the hydrolysis of a MetAP substrate, and its identity as a mycobacterial MetAP was not confirmed by sequencing.

Many dinuclear metallohydrolases[5] play key roles in physiological and pathological processes and often are targets for therapeutics, for instance, MetAP in protein cotranslational modification, dicer in RNA interference,[45] HIV reverse transcriptase in AIDS,[46] and protein phosphatase-1 in cell cycle regulation.[47] Assignment of their physiologically relevant metalloform is often difficult and confusing, but it is critically important for the discovery and development of inhibitors that are effective against cellular enzymes. Initially from high throughput screening, we discovered several classes of unique MetAP inhibitors that can distinguish different metal ions at the enzyme active site.[13-14] These metalloform-selective inhibitors are valuable research tools for the assignment, and here we presented an example of their application to clarification of the native metalloform of *Mt*MetAP1c in an *E. coli* cellular environment. With confirmed inhibitory potency and selectivity on the metalloforms of the purified *Mt*MetAP1c, we characterized these inhibitors for inhibition of MetAP activity from the recombinant *Mt*MetAP1c in live *E. coli* cells. Only the Fe(II)-form selective inhibitors inhibited the cellular MtMetAP1c activity and inhibited the growth of *Mt*MetAP1c-complemented *E. coli* cells, leading to the conclusion that *Mt*MetAP1c is in the Fe(II)-form in an *E. coli* cellular environment. It is intriguing why *Mt*MetAP1c utilizes Fe(II) for catalysis when Ni(II) offers higher catalytic efficiency. One possibility is the higher affinity and easier availability of Fe(II). Expression of *Mt*MetAP1c in *E. coli* probably does not swap the intracellular type of metal utilized by *Mt*MetAP1c in *M. tuberculosis*. For instance, it was demonstrated that *E. coli* peptide deformylase uses Fe(II) as the native metal cofactor, but the *Borrelia burgdorferi* counterpart utilizes Zn(II) after heterologous expression in *E. coli*.[48] Nevertheless, the native metalloform of *Mt*MetAP1c in *M. tuberculosis* remains to be confirmed. Our approach of using *Mt*MetAP1c in *E. coli* cells is an attractive alternative to the direct manipulation of pathogenic organisms for drug discovery that would be accessible to only a selected few due to the dangers they pose.

We presented the first group of small molecule inhibitors for a mycobacterial MetAP enzyme and elucidated their binding characteristics at the enzyme active site. They showed not only potency but also selectivity for different metalloforms and are initial lead compounds for the development of inhibitors of mycobacterial MetAPs as novel anti-TB drugs. Although metalloform selectivity may not be required for effective inhibition of cellular MetAPs, selective inhibition of different metalloforms may be advantageous. Fe(II) is likely the metal used by MetAPs in bacteria such as *E. coli* and *Bacillus*.[15] On the contrary, human type 2 MetAP uses Mn(II) as its physiologically relevant metal cofactor.[49] It is unknown which metal human type 1 MetAP uses for its catalysis, but it is possibly not Fe(II) because free Fe(II) concentration in mammalian cells is low and sequestering iron is a defense mechanism against bacterial infection.[50-51] Metalloform-selectivity may provide a viable strategy for selective inhibition of bacterial MetAP enzymes.

Experimental Section

Materials

The fluorogenic substrate, methionyl aminomethylcoumarin (Met-AMC), was purchased from Bachem Bioscience (King of Prussia, PA). Fluorescent dye resazurin was obtained from Acros Organics (Morris Plains, NJ). MOPS-based rich defined media[17] was acquired from Teknova (Hollister, CA). The *E. coli* strain with an amber mutation in the chromosomal *Ec*MetAP gene[18] was a generous gift from Prof. Frederick Blattner at University of Wisconsin. The genomic DNA of *M. tuberculosis* H37Rv was kindly provided by Prof. Scott Franzblau at University of Illinois at Chicago. Triazole inhibitors were purchased from ChemBridge (San Diego, CA) with purity >95%, and their purity and identity were confirmed by LC-MS and NMR.

Preparation of *Mt*MetAP1c protein

The *Mt*MetAP1c gene (locus_tag Rv2861c) was cloned by PCR from the genomic DNA of *M. tuberculosis* H37Rv, using primers 5′-ggatcaccaGCTAGCatgcctagtcgtaccgcg-3′ (forward) and 5′-agcactcGAATTCtacagacaggtcag-3′ (reverse) (restriction sites are in capital letters). The DNA fragment was digested with *Nhe*I and *Eco*RI and cloned into an *E. coli* expression vector pGEMEX-1 (Promega, Madison, WI) as pGEMEX1-*Mt*MetAP1c for expression under the control of a T7 promoter. The final recombinant protein *Mt*MetAP1c has three residues MAS added to its N-terminus. The recombinant plasmid was introduced into the *E. coli* BL21(DE3) strain for expression. A single colony was grown overnight in a 5 mL LB medium with 100 μg/mL ampicillin at 37 °C, and the overnight culture was used to inoculate 1 L of LB medium containing 100 μg/mL ampicillin. The culture grew at 37 °C, and protein expression was induced by adding IPTG when OD_{600} reached 0.6-0.8. Afterward, cells were shaken at 16 °C for 20 hr before harvesting by centrifugation. A resuspension buffer (50 mM Tris, pH 8.0, 150 mM NaCl, 5 mM EDTA) was used to suspend cell pellets, and the cell suspension was stored at -20 °C. Frozen cells after thawing were broken by three consecutive passes through French Press at 1000 psi. The supernatant was collected from centrifugation at 20,000 rpm for 30 minutes and loaded to a Q-Sepharose column, which was equilibrated with buffer A (50 mM Tris, pH 8.0). The proteins were eluted with a linear gradient of NaCl from 0 to 1 M. *Mt*MetAP1c appeared in the flow-through fractions. Ammonium sulfate was added into the combined fractions in a step-wised manner. The majority of *Mt*MetAP1c was precipitated when ammonium sulfate was 40% saturated. The pellet was resuspended in buffer A, and the mixture was loaded to a desalting column (5-mL HiTrap) to remove ammonium sulfate. Chelex-100 resin (BioRad, Hercules, CA) was added to the combined active fractions, and the mix was shaken at 4 °C for 2 hr. The sample was filtered to remove the resin, loaded to a desalting column, and eluted with buffer B (50 mM Tris, pH 8.0, 150 mM NaCl, which was pre-treated

with Chelex-100). The *Mt*MetAP1c in apoform was verified by hydrolysis of Met-AMC in the presence and absence of divalent metals, and no activity was detected before metal was added.

Assays for catalysis and inhibition of *Mt*MetAP1c as a purified enzyme

Enzymatic activity of *Mt*MetAP1c was monitored by fluorescence (λ_{ex} 360 nm, λ_{em} 460 nm) on a SpectraMax Gemini XPS plate reader (Molecular Devices, Sunnyvale, CA), following hydrolysis of Met-AMC at room temperature as described.[8, 19] All kinetic experiments were carried out on 384-well plates. Each well contained 80 μL assay mixture with 50 mM MOPS, pH 7.5, 100 μM Met-AMC, 0.5 μM apoenzyme, and metal ions (50 μM $FeCl_2$ with 100 μM ascorbic acid, 10 μM $CoCl_2$, 20 μM $MnCl_2$, or 20 μM $NiCl_2$). For IC_{50} determination, the inhibitors were tested at 6 or more serially diluted concentrations. The IC_{50} values were calculated from non-linear regression curve fitting of percent inhibitions as a function of inhibitor concentrations. For metal titration, each well contained 80 μL assay mixture with 50 mM MOPS, pH 7.5, 100 μM Met-AMC, 0.5 μM apoenzyme, and increasing concentrations of metal ions ($FeCl_2$ with twice the concentration of ascorbic acid, $CoCl_2$, $MnCl_2$, $NiCl_2$ or $ZnCl_2$). The initial velocity values were converted to specific activity values and plotted against increasing concentrations of the metal. For determination of kinetic parameters, the 80 μL assay mixture per well contained 50 mM MOPS, pH 7.5, 0.5 μM apoenzyme, metal ions (50 μM $FeCl_2$ with 100 μM ascorbic acid, 10 μM $CoCl_2$, 20 μM $MnCl_2$, or 20 μM $NiCl_2$), and increasing concentrations of Met-AMC. The initial rates were plotted with the corresponding substrate concentrations, and the curve was fitted with the Michaelis-Menten equation to obtain K_m and k_{cat}. We used an improved model of the multiple independent binding sites to calculate the binding affinity K_d, taking into consideration the amount of functional enzyme, which we described recently.[20] Briefly, the initial rate of hydrolysis was plotted against increasing concentrations of Co(II) at two *Mt*MetAP1c protein concentrations (20 μM and 0.5 μM) and fit with the model via an iterative process to obtain an accurate protein concentration. For K_d determination of the various divalent metals to *Mt*MetAP1c, the titration curves were generated using the calculated apoenzyme of 0.54 μM in 50 mM MOPS, pH 7.5, 200 μM Met-AMC and increasing concentrations of either $CoCl_2$, $MnCl_2$, $NiCl_2$ or $FeCl_2$. In the case of $FeCl_2$, ascorbic acid was added at double the concentration of $FeCl_2$. An iterative process was allowed to proceed until K_d and functional enzyme concentration values converged after a few cycles.

Complementation of the essential function of *Ec*MetAP with *Mt*MetAP1c in *E. coli*

To construct a plasmid with expression of the *Mt*MetAP1c gene under the control of an IPTG-inducible *tac* promoter, an *Nde*I/*Bam*HI fragment was cut from pGEMEX1-*Mt*MetAP1c and cloned into pFLAGCTC (Sigma, Saint Louis, MO) as pFLAGCTC-*Mt*MetAP1c. Similarly, the *Ec*MetAP gene was cloned into the pFLAGCTC plasmid as pFLAGCTC-*Ec*MetAP. Both the parent plasmid pFLAGCTC and the plasmid pFLAGCTC-*Ec*MetAP were used as controls. The plasmids were introduced into the *E. coli* cells with an amber mutation in the chromosomal *Ec*MetAP gene. A special MOPS-based rich defined medium[18, 21] was used in combination with kanamycin, ampicillin, L-arabinose, D-glucose, and IPTG. The cells were cultured in the liquid medium or on agar plates prepared with the medium.

Inhibition of cellular *Mt*MetAP1c activity

The above-mentioned pFLAGCTC-*Mt*MetAP1c-transformed *E. coli* cells (*Mt*MetAP1c-complemented cells) were used to establish the cellular *Mt*MetAP1c activity assay. Bacterial cells were allowed to grow to the exponential phase, harvested and washed twice with water. The final cell pellet was resuspended in 10 mM $CaCl_2$, 100 mM Tris, pH 7.5, and then an equal volume of glycerol was added. The cell suspension was aliquoted and kept at -80 °C for storage. For the cellular *Mt*MetAP1c activity assay, the cell suspension was diluted with 10 mM $CaCl_2$, and 100 mM Tris, pH 7.5. The cells, substrate Met-AMC, and inhibitor at 12 serially

diluted concentrations were combined in wells of a 384-well plate. The final assay volume was 80 μl with 150 μM Met-AMC, 5 mM $CaCl_2$, and 50 mM Tris, pH 7.5. Increase of the fluorescent product was monitored via fluorescence (λ_{ex} 360 nm, λ_{em} 460 nm) at room temperature every 2 min for 6-8 hr. The IC_{50} values were calculated from the rate of substrate hydrolysis.[15]

Inhibition of *Mt*MetAP1c-complemented *E. coli* cell growth

Inhibition of bacterial growth was carried out by using the *Mt*MetAP1c-complemented *E. coli* cells. The experiments were performed in a similar way as previously reported with minor modifications.[14-15] The assay was carried out on 384-well opaque plates containing 12 serially diluted concentrations for each inhibitor (40 μL per well) with the highest final concentration of 1 mM in the assay. A suspension of bacterial cells was prepared from agar plates containing rich defined media with 0.2% glucose, 50 μg/mL kanamycin and 100 μg/mL ampicillin grown to the exponential phase, which was used to inoculate a second culture batch. This ensured that the survival of the cells was due to *Mt*MetAP1c complementation rather than residual endogenous *Ec*MetAP. The suspension was adjusted to 0.5 McFarland optical density [22] and then further diluted by 1000 fold in the same medium containing 100 mM Tris, pH 7.5, and 225 μM resazurin. Cells were dispensed into the microplate (40 μL per well) by a Multidrop Combi reagent dispenser (Thermo Scientific, Waltham, MA). The conversion from resazurin to resofurin was monitored kinetically by fluorescence (λ_{ex} 530 nm and λ_{em} 590 nm) using a SpectraMax Gemini XPS plate reader. Fluorescence kinetic experiments were carried out for 10 hr at 37 °C, with readings taken every 5 min. Signal intensities at time points along the exponential phase of the growth curve corresponding to 50-85% of total intensity of an uninhibited sample were averaged and converted to percent inhibitions to calculate IC_{50} values by non-linear regression curve fitting.

Crystallization and data collection

Crystals of the enzyme-inhibitor complexes were obtained independently by a hanging-drop vapor-diffusion method at room temperature. Each of the inhibitors (**4**, **7**, and **8**; 100 mM in DMSO) was added to concentrated metalated enzyme (10 mg/mL, 0.32 mM protein; 2 mM metal) in 50 mM Tris, pH 8.0, 150 mM NaCl and the molar ratio of inhibitor to *Mt*MetAP1c was 5:1 or 10:1. The enzyme/inhibitor mixture was mixed with a reservoir buffer in a 1:1 ratio. The reservoir buffer was 100 mM Bis-Tris, pH 5.5, 1.1 M NH_4SO_4, and 50 mM NaCl for **4**; 100 mM Bis-Tris, pH 5.5, 1.4 M NH_4SO_4, and 15% glycerol for **7**; and 100 mM Bis-Tris, pH 5.5, 1.3 M NH_4SO_4, and 15% glycerol for **8**. Diffraction data were collected at the Advanced Photon Source, Argonne National Laboratory (beamline 19BM) and processed with HKL3000.[23-24] All of the crystals belong to space group $P6_3$. One molecule is in the asymmetric unit.

Structural solution and refinement

The structures were solved by molecular replacement with MolRep[25] in CCP4[26] with CCP4i interface,[27] using the previously published *Mt*MetAP1c structure (PDB code 1YJ3)[4] as the search model. The structure was refined with REFMAC5[28] with iterative model building using WinCoot.[29] The refinement was monitored with 5% of the reflections set aside for R_{free} factor analysis throughout the whole refinement process. Electron density was clear for all residues except a few residues at the N-terminus, and residues from the second (P2) in the native protein to the end (L285) were modeled. Comparison of structures and generation of structural drawings were carried out by using PyMOL.[30] Statistic parameters in data collection and structural refinement are shown in Table 3. Atomic coordinates and structure factors for the three structures were deposited in the Protein Data Bank.

Acknowledgments

This work was supported by National Institutes of Health Grant R01 AI065898 (to Q.-Z. Y.). We thank Prof. Frederick Blattner for the *E. coli* strain with an amber mutation at chromosomal *Ec*MetAP gene and Prof. Scott Franzblau for the genomic DNA of *M. tuberculosis* H37Rv. We thank the staffs at Structural Biology Center of the Advanced Photon Source, Argonne National Laboratory (beamline 19BM) for assistance with data collection.

References

1. Fauci AS. Multidrug-Resistant and Extensively Drug-Resistant Tuberculosis: The National Institute of Allergy and Infectious Diseases Research Agenda and Recommendations for Priority Research. J Infect Dis 2008;197:1493–1498. [PubMed: 18426366]
2. Vaughan MD, Sampson PB, Honek JF. Methionine in and out of proteins: targets for drug design. Curr Med Chem 2002;9:385–409. [PubMed: 11860363]
3. Giglione C, Boularot A, Meinnel T. Protein N-terminal methionine excision. Cell Mol Life Sci 2004;61:1455–1474. [PubMed: 15197470]
4. Addlagatta A, Quillin ML, Omotoso O, Liu JO, Matthews BW. Identification of an SH3-binding motif in a new class of methionine aminopeptidases from Mycobacterium tuberculosis suggests a mode of interaction with the ribosome. Biochemistry 2005;44:7166–7174. [PubMed: 15882055]
5. Wilcox DE. Binuclear Metallohydrolases. Chem Rev 1996;96:2435–2458. [PubMed: 11848832]
6. Lowther WT, Matthews BW. Metalloaminopeptidases: common functional themes in disparate structural surroundings. Chem Rev 2002;102:4581–4608. [PubMed: 12475202]
7. D'Souza VM, Holz RC. The methionyl aminopeptidase from Escherichia coli can function as an iron (II) enzyme. Biochemistry 1999;38:11079–11085. [PubMed: 10460163]
8. Li JY, Chen LL, Cui YM, Luo QL, Li J, Nan FJ, Ye QZ. Specificity for inhibitors of metal-substituted methionine aminopeptidase. Biochem Biophys Res Commun 2003;307:172–179. [PubMed: 12849997]
9. Lowther WT, Matthews BW. Structure and function of the methionine aminopeptidases. Biochim Biophys Acta 2000;1477:157–167. [PubMed: 10708856]
10. Luo QL, Li JY, Liu ZY, Chen LL, Li J, Qian Z, Shen Q, Li Y, Lushington GH, Ye QZ, Nan FJ. Discovery and structural modification of inhibitors of methionine aminopeptidases from Escherichia coli and Saccharomyces cerevisiae. J Med Chem 2003;46:2631–2640. [PubMed: 12801227]
11. Schiffmann R, Heine A, Klebe G, Klein CD. Metal ions as cofactors for the binding of inhibitors to methionine aminopeptidase: A critical view of the relevance of in vitro metalloenzyme assays. Angew Chem Int Ed Engl 2005;44:3620–3623. [PubMed: 15880695]
12. Douangamath A, Dale GE, D'Arcy A, Almstetter M, Eckl R, Frutos-Hoener A, Henkel B, Illgen K, Nerdinger S, Schulz H, Mac Sweeney A, Thormann M, Treml A, Pierau S, Wadman S, Oefner C. Crystal structures of Staphylococcusaureus methionine aminopeptidase complexed with keto heterocycle and aminoketone inhibitors reveal the formation of a tetrahedral intermediate. J Med Chem 2004;47:1325–1328. [PubMed: 14998322]
13. Ye QZ, Xie SX, Huang M, Huang WJ, Lu JP, Ma ZQ. Metalloform-selective inhibitors of escherichia coli methionine aminopeptidase and X-ray structure of a Mn(II)-form enzyme complexed with an inhibitor. J Am Chem Soc 2004;126:13940–13941. [PubMed: 15506752]
14. Wang WL, Chai SC, Huang M, He HZ, Hurley TD, Ye QZ. Discovery of inhibitors of Escherichia coli methionine aminopeptidase with the Fe(II)-form selectivity and antibacterial activity. J Med Chem 2008;51:6110–6120. [PubMed: 18785729]
15. Chai SC, Wang WL, Ye QZ. FE(II) Is the Native Cofactor for Escherichia coli Methionine Aminopeptidase. J Biol Chem 2008;283:26879–26885. [PubMed: 18669631]
16. Zhang X, Chen S, Hu Z, Zhang L, Wang H. Expression and Characterization of Two Functional Methionine Aminopeptidases from Mycobacterium tuberculosis H37Rv. Curr Microbiol 2009;59:520–525. [PubMed: 19688379]
17. Neidhardt FC, Bloch PL, Smith DF. Culture medium for enterobacteria. J Bacteriol 1974;119:736–747. [PubMed: 4604283]
18. Herring CD, Blattner FR. Conditional lethal amber mutations in essential Escherichia coli genes. J Bacteriol 2004;186:2673–2681. [PubMed: 15090508]

19. Yang G, Kirkpatrick RB, Ho T, Zhang GF, Liang PH, Johanson KO, Casper DJ, Doyle ML, Marino JP Jr, Thompson SK, Chen W, Tew DG, Meek TD. Steady-state kinetic characterization of substrates and metal-ion specificities of the full-length and N-terminally truncated recombinant human methionine aminopeptidases (type 2). Biochemistry 2001;40:10645–10654. [PubMed: 11524009]
20. Chai SC, Lu JP, Ye QZ. Determination of binding affinity of metal cofactor to the active site of methionine aminopeptidase based on quantitation of functional enzyme. Anal Biochem 2009;395:263–264. [PubMed: 19712663]
21. Herring CD. Introduction of conditional lethal amber mutations in Escherichia coli. Methods Mol Biol 2008;416:323–334. [PubMed: 18392977]
22. National Committee for Clinical Laboratory Standards. Methods for dilution antimicrobial susceptibility tests for bacteria that grow aerobically, Approved standard M7-A4. National Committee for Clinical Laboratory Standards; Wayne, PA: 2000.
23. Otwinowski, Z.; Minor, W. Processing of X-ray Diffraction Data Collected in Oscillation Mode. In: Carter, CW.; Sweet, RM., editors. Methods in Enzymology. Vol. 276. Academic Press; New York: 1997. p. 307-326.
24. Minor W, Cymborowski M, Otwinowski Z, Chruszcz M. HKL-3000: the integration of data reduction and structure solution--from diffraction images to an initial model in minutes. Acta Crystallogr D Biol Crystallogr 2006;62:859–866. [PubMed: 16855301]
25. Vagin A, Teplyakov A. MOLREP: an Automated Program for Molecular Replacement. J Appl Crystallogr 1997;30:1022–1025.
26. Collaborative Computational Project Number 4. The CCP4 Suite: Programs for Protein Crystallography. Acta Cryst 1994;D50:760–763.
27. Potterton E, Briggs P, Turkenburg M, Dodson E. A graphical user interface to the CCP4 program suite. Acta Crystallogr D Biol Crystallogr 2003;59:1131–1137. [PubMed: 12832755]
28. Murshudov GN, Vagin AA, Dodson EJ. Refinement of macromolecular structures by the maximum-likelihood method. Acta Crystallogr D Biol Crystallogr 1997;53:240–255. [PubMed: 15299926]
29. Emsley P, Cowtan K. Coot: model-building tools for molecular graphics. Acta Crystallogr D Biol Crystallogr 2004;60:2126–2132. [PubMed: 15572765]
30. DeLano, WL. The PyMOL Molecular Graphics System. 2002. on World Wide Web http://www.pymol.org
31. Frottin F, Martinez A, Peynot P, Mitra S, Holz RC, Giglione C, Meinnel T. The proteomics of N-terminal methionine cleavage. Mol Cell Proteomics 2006;5:2336–2349. [PubMed: 16963780]
32. Chang SY, McGary EC, Chang S. Methionine aminopeptidase gene of Escherichia coli is essential for cell growth. J Bacteriol 1989;171:4071–4072. [PubMed: 2544569]
33. Oefner C, Douangamath A, D'Arcy A, Hafeli S, Mareque D, Mac Sweeney A, Padilla J, Pierau S, Schulz H, Thormann M, Wadman S, Dale GE. The 1.15A crystal structure of the Staphylococcus aureus methionyl-aminopeptidase and complexes with triazole based inhibitors. J Mol Biol 2003;332:13–21. [PubMed: 12946343]
34. Xie SX, Huang WJ, Ma ZQ, Huang M, Hanzlik RP, Ye QZ. Structural analysis of metalloform-selective inhibition of methionine aminopeptidase. Acta Crystallogr D Biol Crystallogr 2006;62:425–432. [PubMed: 16552144]
35. Krissinel E, Henrick K. Inference of macromolecular assemblies from crystalline state. J Mol Biol 2007;372:774–797. [PubMed: 17681537]
36. Krissinel E. Crystal contacts as nature's docking solutions. J Comput Chem 2010;31:133–143. [PubMed: 19421996]
37. Watterson SJ, Mitra S, Swierczek SI, Bennett B, Holz RC. Kinetic and spectroscopic analysis of the catalytic role of H79 in the methionine aminopeptidase from Escherichia coli. Biochemistry 2008;47:11885–11893. [PubMed: 18855426]
38. Huang M, Xie SX, Ma ZQ, Hanzlik RP, Ye QZ. Metal mediated inhibition of methionine aminopeptidase by quinolinyl sulfonamides. Biochem Biophys Res Commun 2006;339:506–513. [PubMed: 16300729]
39. You C, Lu H, Sekowska A, Fang G, Wang Y, Gilles AM, Danchin A. The two authentic methionine aminopeptidase genes are differentially expressed in Bacillus subtilis. BMC Microbiol 2005;5:57. [PubMed: 16207374]

40. Chen X, Chong CR, Shi L, Yoshimoto T, Sullivan DJ Jr, Liu JO. Inhibitors of Plasmodium falciparum methionine aminopeptidase 1b possess antimalarial activity. Proc Natl Acad Sci U S A 2006;103:14548–14553. [PubMed: 16983082]
41. Miller CG, Kukral AM, Miller JL, Movva NR. pepM is an essential gene in Salmonella typhimurium. J Bacteriol 1989;171:5215–5217. [PubMed: 2670909]
42. Li X, Chang YH. Amino-terminal protein processing in Saccharomyces cerevisiae is an essential function that requires two distinct methionine aminopeptidases. Proc Natl Acad Sci U S A 1995;92:12357–12361. [PubMed: 8618900]
43. Needleman SB, Wunsch CD. A general method applicable to the search for similarities in the amino acid sequence of two proteins. J Mol Biol 1970;48:443–453. [PubMed: 5420325]
44. Narayanan SS, Ramanujan A, Krishna S, Nampoothiri KM. Purification and Biochemical Characterization of Methionine Aminopeptidase (MetAP) from Mycobacterium smegmatis mc(2) 155. Appl Biochem Biotechnol 2008;151:512–521. [PubMed: 18594775]
45. Macrae IJ, Zhou K, Li F, Repic A, Brooks AN, Cande WZ, Adams PD, Doudna JA. Structural basis for double-stranded RNA processing by Dicer. Science 2006;311:195–198. [PubMed: 16410517]
46. Davies JF 2nd, Hostomska Z, Hostomsky Z, Jordan SR, Matthews DA. Crystal structure of the ribonuclease H domain of HIV-1 reverse transcriptase. Science 1991;252:88–95. [PubMed: 1707186]
47. Maynes JT, Bateman KS, Cherney MM, Das AK, Luu HA, Holmes CF, James MN. Crystal structure of the tumor-promoter okadaic acid bound to protein phosphatase-1. J Biol Chem 2001;276:44078–44082. [PubMed: 11535607]
48. Nguyen KT, Wu JC, Boylan JA, Gherardini FC, Pei D. Zinc is the metal cofactor of Borrelia burgdorferi peptide deformylase. Arch Biochem Biophys 2007;468:217–225. [PubMed: 17977509]
49. Wang J, Sheppard GS, Lou P, Kawai M, Park C, Egan DA, Schneider A, Bouska J, Lesniewski R, Henkin J. Physiologically relevant metal cofactor for methionine aminopeptidase-2 is manganese. Biochemistry 2003;42:5035–5042. [PubMed: 12718546]
50. Payne SM. Iron acquisition in microbial pathogenesis. Trends Microbiol 1993;1:66–69. [PubMed: 8044465]
51. Wooldridge KG, Williams PH. Iron uptake mechanisms of pathogenic bacteria. FEMS Microbiol Rev 1993;12:325–348. [PubMed: 8268005]

Abbreviations

MetAP	methionine aminopeptidase
*Ec*MetAP	*E. coli* methionine aminopeptidase
*Mt*MetAP1c	*M. tuberculosis* methionine aminopeptidase type 1c
Met-AMC	methionyl aminomethylcoumarin

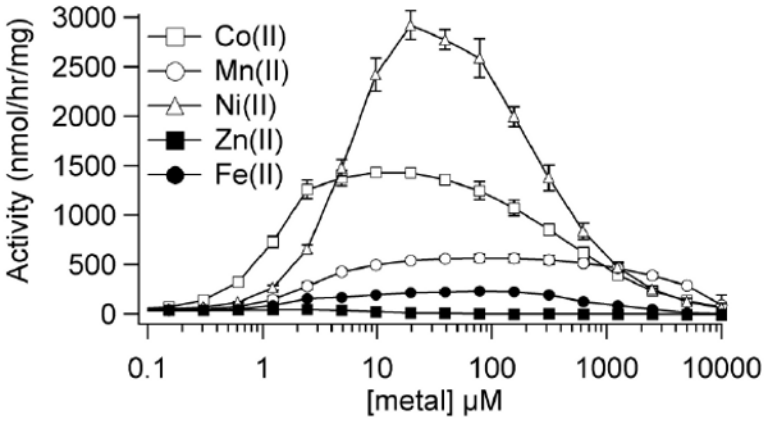

Figure 1.
Activation of *Mt*MetAP1c apoenzyme by divalent metals.

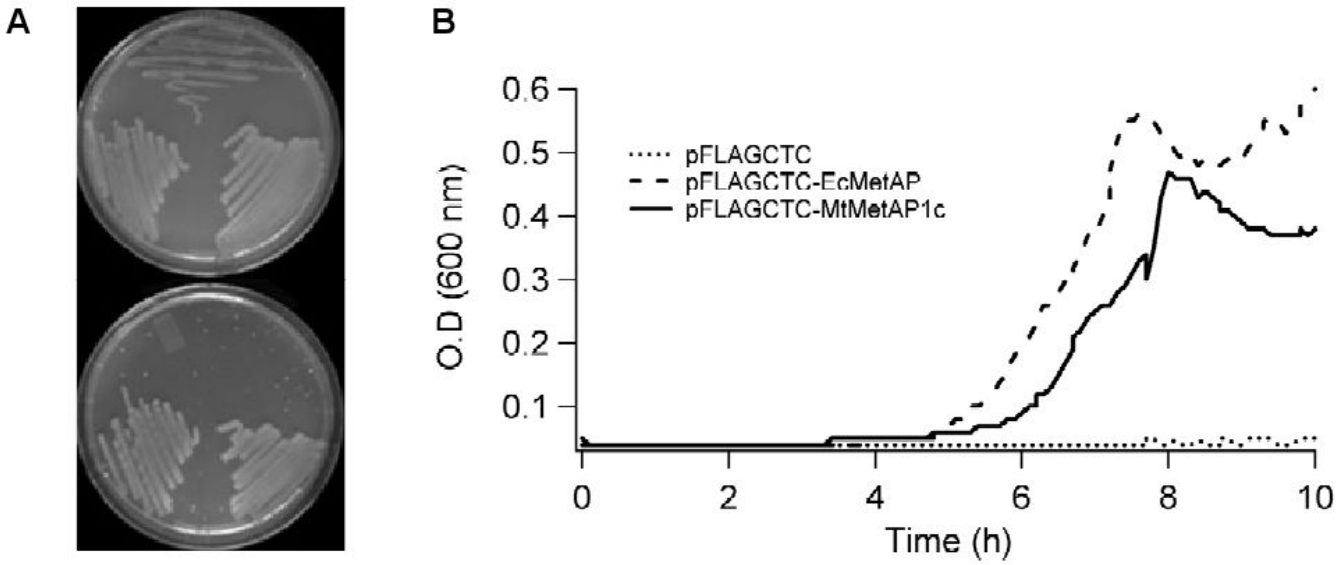

Figure 2.

Complementation of *Ec*MetAP function by *Mt*MetAP1c. **A**. *E. coli* cells carrying an amber mutation in chromosomal *Ec*MetAP gene were streaked on agar plates with glucose (bottom plate) or with arabinose (to plate). Each plate displays cells containing pFLAGCTC (top), pFLAGCTC-*Mt*MetAP1c (bottom left) or pFLAGCTC-*Ec*MetAP (bottom right). **B**. Growth of the *E. coli* cells in liquid medium supplemented with glucose.

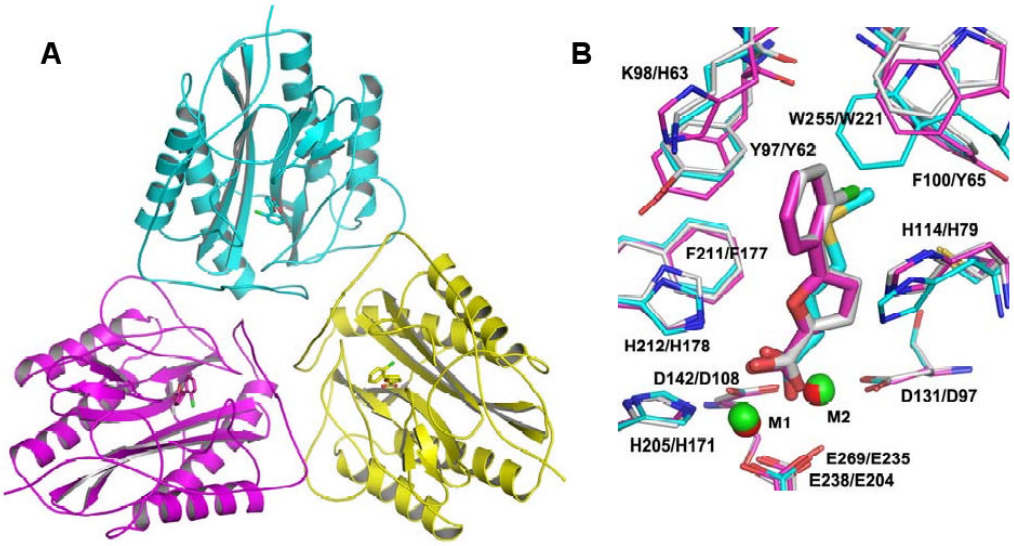

Figure 3.

Structure of *Mt*MetAP1c in the Mn(II)-form in complex with the Mn(II)-form selective inhibitor **4. A**. Trimeric arrangement in crystal. Inhibitor **4** at the active site is shown as sticks. The three molecules of MtMetAP1c were colored cyan, magenta and yellow, respectively. **B**. Overlay of this structure with *Ec*MetAP in complex with the same inhibitor (carbon magenta, pdb 1XNZ) and with the same protein in complex with methionine (carbon cyan, pdb 1YJ3). Only residues (thin sticks) surrounding the ligands (thick sticks) at the active site are shown. Non-carbon atoms are colored oxygen red, nitrogen blue, sulfur yellow, and chlorine green. Mn(II) (green) and Co(II) (red) ions are shown as spheres. For residue labeling, the first is for *Mt*MetAP1c and the second for *Ec*MetAP.

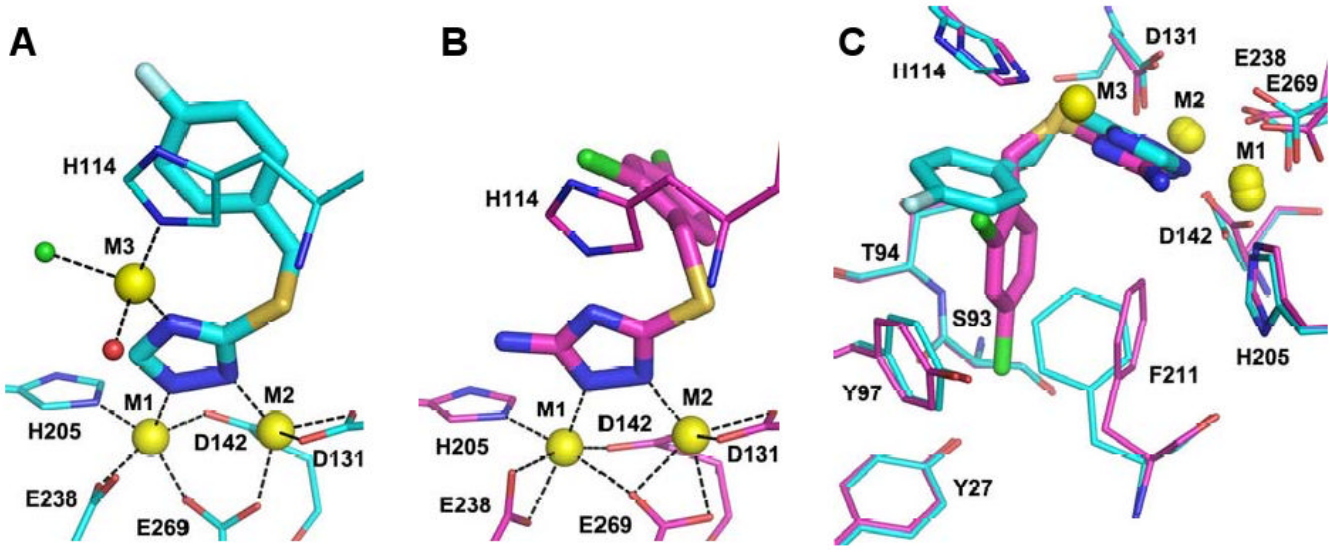

Figure 4.

Structures of *Mt*MetAP1c in the Ni(II)-form in complex with the Co(II)- and Ni(II)-form selective inhibitors **7** and **8. A**. Trimetalated active site with **7** bound. Inhibitor is shown as thick sticks and the protein residues as thin sticks (carbon cyan, oxygen red, nitrogen blue, sulfur yellow, and fluorine pale). Ni(II) ions (yellow) are shown as large spheres, and water (red) and chlorine ion (green) are shown as small spheres. Metal coordination is shown as dashed lines. **B**. Dimetalated active site with **8** bound. Same color scheme, except carbon magenta and chlorine green. **C**. Comparison of the bound conformations of **7** and **8**. For clarity, only selected protein residues are shown.

Table 1

Binding and activation of *Mt*MetAP1c by different metals [a]

	Fe(II)	Ni(II)	Co(II)	Mn(II)
K_d, μM	0.15	1.41	0.13	0.76
K_m, μM	349	141	232	192
k_{cat}, sec^{-1}	0.015	0.093	0.054	0.020
k_{cat}/K_m, $M^{-1}sec^{-1}$	41.6	659	232	107

[a] K_d is the dissociation constant. K_m and k_{cat} are the Michaelis–Menten constants, and they were obtained with Fe(II) at 50 μM, Ni(II) and Mn(II) at 20 μM, and Co(II) at 10 μM.

Table 2

Inhibition of enzymatic activities of purified and cellular *Mt*MetAP1c and inhibition of cell growth of *Mt*MetAP1c-complemeted *E. coli* by metalloform-selective inhibitors [a]

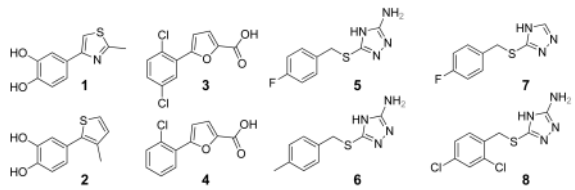

Cmpd	Purified Enzyme [b]				Cellular Enzyme [c]	Bacterial Growth [d]
	Fe(II)	Ni(II)	Co(II)	Mn(II)		
1	3.6	104	76	37	20	208
2	1.4	60	38	14	35	89.5
3	>500	>500	>500	14	623	>1000
4	>500	>500	>500	16	N.D.[e]	N.D.
5	>500	1.3	0.74	18	121	>1000
6	>500	2.5	0.69	26	281	>1000
7	>500	0.58	2.0	143	N.D.	N.D.
8	40	0.24	0.26	2.0	N.D.	N.D.

[a] IC_{50} values are expressed in μM.

[b] Purified enzymes were reconstituted by activating the apoenzyme with different divalent cations [Fe(II), 50 μM; Ni(II) and Mn(II), 20 μM; Co(II), 10 μM)].

[c] Cellular enzyme was the recombinant *Mt*MetAP1c expressed in *E. coli* cells lacking endogenous *Ec*MetAP.

[d] Growth of *E. coli* cells with the recombinant *Mt*MetAP1c was monitored.

[e] Not determined.

Table 3

X-ray data collection and refinement statistics

Inhibitor	**4**	**7**	**8**
Inhibitor code	FCD	T03	T07
PDB code	3IU7	3IU8	3IU9
Metal ion	2 Mn(II)	3 Ni(II)	2 Ni(II)
Cell Parameters			
space group	$P6_3$	$P6_3$	$P6_3$
a (Å)	106.4	105.7	106.2
b (Å)	106.4	105.7	106.2
c (Å)	50.4	50.4	50.8
α (deg)	90	90	90
β (deg)	90	90	90
γ (deg)	120	120	120
X-ray Data Collection			
Resolution range (Å) [a]	50-1.40 (1.42-1.40)	50-1.85 (1.88-1.85)	50-1.75 (1.78-1.75)
Collected reflections	642,578	304,665	301,490
Unique reflections	64,180	27,549	32,971
Completeness (%) [a]	99.9 (100)	99.5 (90.5)	99.5 (92.2)
$I/\sigma(I)$ [a]	43.8 (9.4)	23.3 (3.8)	59.8 (15.7)
R_{merge} (%) [a]	4.5 (21.5)	15.6 (71.4)	7.8 (17.5)
Refinement Statistics			
R (%)	17.1	16.5	16.4
R_{free} (%)	19.0	20.0	19.5
R.m.s.d. bonds (Å)	0.031	0.028	0.028
R.m.s.d. angles (°)	2.52	1.97	2.31
No. of solvent molecules	249	162	193
<B> protein ($Å^2$)	11.0	14.4	14.1
<B> inhibitor ($Å^2$)	9.5	21.4	12.5
<B> water ($Å^2$)	18.6	19.2	19.7

[a] Values given in parentheses correspond to the outer shell of data.